Received: 6 November 2018 | Revised: 21 February 2019 | Accepted: 12 March 2019

DOI: 10.1002/ese3.336

RESEARCH ARTICLE

Energy Science & Engineering
Open Access

Impact of extreme events on conversion efficiency of wave energy converter

Tilottama Chakraborty | **Mrinmoy Majumder**

School of Hydro-informatics Engineering, National Institute of Technology Agartala, Agartala, Tripura, India

Correspondence
Mrinmoy Majumder, School of Hydro-informatics Engineering, National Institute of Technology Agartala, Agartala, Tripura, India.
Email: mmajumder15@gmail.com

Abstract

Uncontrolled high emission of greenhouse gases due to the use of fossil fuels has high impact on global warming. Due to this global warming, the earth's temperature is increasing and consequently has changed the patterns of various natural phenomena such as wave height and wind speed**.** Wave power energy resources are ideal alternative to reduce the effects of global warming and climate change. One of the major obstacles lies in the fact that the occurrence of extreme events can jeopardize the wave power plant suspended in the ocean waves. In order to better understand the impact of extreme events on the wave energy generation, a comprehensive analysis of utilization efficiency of wave energy converters with respect to extreme events was conducted in the present investigation with the help of utilization efficiency function (UEF) as an indicative index function. The effect of the extreme events was simulated by the polynomial neural network (PNN) architectures, and change in UEF in the future scenarios was noted. According to the results, the maximum impact on the utilization efficiency of the WEC was observed in the time slab of 2050-2060, where 5.1% change in utilization efficiency was observed.

KEYWORDS

climate change impacts, extreme events, group method of data handling, polynomial neural networks, wave energy converter

1 | INTRODUCTION

Wave energy has the capacity to supply total energy demand of the world.[1,2,3] Wave energy evaluation comes under two categories. The first category focuses on the climatological, that is, wave data, and the second category considered the configuration and efficiency of wave energy converter,[4,6] infrastructure, cost, and other constraints with climatological factors.[7] In the past few years, numerous studies have been done to evaluate the wave energy around the world.[8,9,10] Among others, Lin et al[11] carried out a study to determine the more eligible location for wave energy production in China. Chakraborty et al[12] develop a model to identify the best suitable location for obtaining the maximum utilization potential of a wave energy converter. In another study, conducted by Zanous et al,[13] wave energy potential and the suitable location selection for installing the wave energy converter were also investigated using European Centre for Medium-Range Weather Forecasts (ECMWF) along the southern coast and islands of Iran. Among all the studies mentioned, the impact of extreme events on the wave energy converter has not been included.

However, as with the other alternative sources of energy, variations in regular climatic pattern due to the global

warming affect the wave energy potential and average wave power level[3] of a region. The wave energy potential of a region depends on height of the waves which again depend on speed, duration, and fetch of the wind flowing in that region.[14,15,16] According to Sisco et al,[17] changes in climatic trend have impacted the normal pattern of climatic parameters such as wind speed and its duration in many parts of the world. As a result, potential of wave energy has also changed on those locations.[18,19] Many papers had highlighted different indication of change in characteristic of the ocean due to the change in regular pattern of the climatic parameters. If ocean characteristics changes, then it will impact the wave height and subsequently wave power level of the region.

The climatic trends of significant wave height (SWH) and wave power density (WPD) have a significant impact on the wave energy development.[20,21,22,23,24] The long-term trend of SWH also has a close relationship with the extreme events and climate change.[25,26,27,28,29,30]

The studies described in previous paragraphs depicted that due to the change in climate, in recent years, different physical, chemical, and hydrodynamic characteristics of the ocean have changed.[31,32,33,34,35,36] As a result, the necessity of numerical models, developed for the estimation of wave height, specially during the occurrence of extreme events and simulation of response from the wave converters installed for utilization of wave energy potential, has raised significantly.

The extreme sea state is defined as the amalgamation of the extreme wave, wind, and current events which are generally the input parameters of device response models. The extreme event is identified by the recurrence interval or return period of the events which is also the inverse of the probability of occurrence of that event. Generally, 30 or more years of data are collected from the in situ measurements of historical records and for each event the return period is estimated. Each wave energy converter (WEC) is designed for a specific return period after which the survivability as well as reliability of performance diminishes. Although there is no specific guideline but considering the average lifetime of a WEC device, such systems are designed for an extreme event which can return only after 50 years.[37]

In recent years, many studies have used cognitive classifiers,[38] vector maps, K-mean clustering, etc. for the identification of the extreme event and to estimate its chance of occurrence. However, as prediction of extreme sea state and the response of WEC depend on multiple factors,[37] high-fidelity numerical models validated by physical experiments are mostly used for the determination of the extreme events and its response by the converters which creates the need to develop a model which can predict the atrocities on a WEC due to an extreme events. Section 1.1 describes the objective and novelty of the present investigation.

1.1 | Objective and novelty

The modeling of either the wave energy potential or the response from the WEC lacks accuracy due to the multiple factors that control these phenomena. Again, not all the factors are equally sensitive in the estimation of such phenomena. In case of wave energy prediction, a minimum variation in steepness of the wave will have a large variation on energy of wave either at the peak or crest. The direction of the wave incident upon the WEC also has an impact on the response received from the WEC but not as acute as in case of a change in the "wave height-to-wave length" ratio. Failure in mechanical, electrical, and civil component of the PCC will yield different responses from the converter for different failures in the same converter. Such multifactor variations are complex to design and result in the inaccuracy of the developed simulation framework. As a result, multi-indicator index-based models are nowadays gaining popularity in the estimation of outcome from a device response framework which depends on multiple parameters.

As UEF is the result of impact from multiple relevant parameters, the estimation of utilization by this function is more accurate compared to any numerical or CFD model. But to be ensured about the reliability of the results from UEF, the output was tested by physical experiments. The accuracy level of the PNN model for the estimation of UEF was found to be equal to 98% which encouraged the authors to apply the same UEF to depict the impact of extreme events on utilization efficiency of a converter for a specific location.

That is why the main objective of the present investigation was to estimate and analyze the impact of extreme events on utilization efficiency of the WEC for a location. The study will also try to examine the potential of UEF in the estimation of impacts from extreme events. Section 2 describes in detail the chronological development of sea state models and its approximations.

2 | LITERATURE REVIEW

Frequency domain dynamic response models are usually used for the determination of sea state and device response. Although such models are successful in prediction of sea state during regular sea condition, it fails to estimate the nonlinearities involved in an irregular wave spectra. As a consequence, many numerical models were designed and implemented for device response and sea state estimations. These models were successful in prediction of nonlinearities including irregular wave patterns but were unsuccessful in simulating the viscosity and wave breaking phenomena. As a result, high-fidelity computational fluid dynamics (CFD) models were developed which were able to estimate irregularity and nonlinearity in the wave spectrum and device

response (which include the difficulties of large variation in wave amplitude, wave breaking, viscosity, and nonlinearities in the power conversion chains (PCC) for which electrical and mechanical failures often occur during the operational phase of a WEC). But for CFD models also, the need of validation of the results requires comparison with physical models where real-life conditions were replicated in laboratory or regulated environment.

In case of physical models, downscaling of independent factors of the physical phenomena determines the accuracy of the results from an experimental setup developed to replicate the phenomena. Generally, the Froude's scaling factor is used for the estimation of the ratio of downscale. The mechanical friction, stiffness, viscosity, and air compression cannot be represented by Froude's scaling equation. For that reason, the physical model is required to be adapted by considering the impacts of factors which cannot be downscaled by the Froude's scaling. However, prediction of wave energy potential by employing multiparametric indicators was also attempted by various authors where selection of location with respect to converter efficiency and available wave energy potential of the region was the main objective.

Such studies include the index proposed by Ghosh et al[39] for the selection of suitable location for the installation of wave power plants considering multiple factors excluding the role of WEC. Although locations were selected for the installation of wave power plants based on wave height, wave period, and many other factors, load on the converters and their nonlinearities was not included in the study. As a result, the suitable locations can be identified but conversion efficiency of WEC cannot be ensured. In 2015, Ghosh et al tried to classify the suitable locations with the help of wave climatic parameters including ocean depth. The result from the study concluded that the wind speed is the most significant parameter compared to other climatic parameters and depth of ocean in selection of location for the installation of wave power plant. In this study also, the role of WEC was not included. Therefore, in 2017, Chakraborty and Majumder tried to identify the location for the installation of wave power plant considering the role of the converters. Not only the nonlinearities of the WEC were represented by the inclusion of relevant factors but also the cost required for the installation, operation, and maintenance of the converters on the location was included in the decision making. Here, prediction of the index from its variables was made by polynomial neural network (PNN) which was a better architecture compared to feedforward neural network[12] for automating the predictive framework. The index was named as utilization efficiency function (UEF).

The sea state and converter efficiency prediction models depend on multiple factors which can be classified into location dependent, converter design, and cost factors. Wave climate and ocean depth vary with locations and so is the wave power level. This variation includes the breaking and viscosity properties of wave and also represents the impacts due to the change in steepness of waves. The nonlinear dynamics in PCC and survivability of WEC can be represented by its design parameters such as efficiency of the mooring structure, hydraulic system, turbine and generators, and shape and size of the buoy. The cost required for the installation, operation, and maintenance of the WEC was included under the cost factors.

Swells created by south/northwesterly can propagate a long distance. Such swells are detrimental for the installation of WEC. The swell generated will have definite impact on the wave energy extraction from a potential location by a WEC.[20,40,41] Swell has the potential to change the wave height, period, and regularity in the wave climate which may result in the irregular pattern of energy production. That is why all these factors or indicators were augmented to produce the utilization efficiency function[42,43] which was used to determine the capacity of converters in utilization of potential wave energy from the selected region. Section 3 explains the procedure adopted to represent the impact of extreme events on the capacity of WEC in extraction of available potential.

3 | METHODOLOGY

In the present investigation, a four-step methodology was adopted to attain the objective of the current analysis. At the first step, the type of converter, location, time slabs, and the climate model were selected. In a previous study, conducted by the authors of the present study (2017), identified Mighty Whale Oscillating Water Column (OWC)[44] type of WEC (Section 3.1.3) in the Kochi location of Kerala (Section 3.1.2) to have the highest utilization capacity among the locations considered in that study. That is why the same location with the same type of converter was utilized in the present investigation for analyzing the extreme event impacts.

The determination of utilization efficiency of converters in extreme sea state impacted by the change in climate is a multifactor approach. The nonlinearities and dynamics involved in such prediction were represented by considering the aggregated function of the relevant indicators selected based on the locational irregularities, nonlinear dynamics in device response, and cost effects. The aggregate function, which is the UEF, was also designed in such a manner that it will include the influence of the indicators as per their significance on device response. Section 3.1 gives a brief description of the UEF model.

The future climatic data were collected from the HadCM3 model for A2 and B2 scenario of IPCC for three future time slabs, that is, 2010-2030, 2031-2070, and 2070-2100. Section 3.1.1 depicts a discussion on the selected climate model along with the justification of utilizing the model for

attaining the objective of the present objective. Table 1 depicts the data collection and calculation followed for deriving the data for the indicators for both present and future scenarios.

The wave height depends on speed, duration, and fetch of wind flowing through the region and thereby representing the impact of swell in the ocean. The climate models, which are developed to estimate the magnitude of climatic parameters for the future time slabs, do not predict wave height as it is not a climatic parameter. That is why in the second step of the present investigation, a simulation model was developed to estimate the wave height as a function of wind speed. The data (Table 1) of the baseline scenario or the current time slab were used to train the model, and the input data from the future time slabs as predicted by the selected climate model were fed into the simulation model which predicted the magnitude of wave height for the same time slabs. Duration and fetch were assumed to be constant and equal to the observed monthly value of the baseline scenario measured in the selected region. The results from the simulation model were validated with the help of the projection of wave height data from inverse FORM technique.[45] Section 3.2 portrays a brief explanation of the model.

TABLE 1 Description and source of data collection of the indicators considered in the present investigation for both present and future time slabs

Name of parameter	Source/Method for data collection
Locational aspects	
Significant Wave Height (m)(w_1)[a]	Present (2009-17): http://www.buoyweather.com Future (2019 to 2070): http://worldclim.org/ (IPCC A2 and B2 Scenario)
Wave Amplitude (m) (w_2)	The magnitude of energy transported by a wave is associated with the amplitude of the wave. A high energy wave is distinguished by a high amplitude; a low energy wave is recognized by a low amplitude. The energy transported by the wave is directly proportional to the square of the amplitude
Wave Period (w_3)[a]	Present (2009-17): http://www.buoyweather.com Future (2019 to 2070): http://worldclim.org/ (IPCC A2 and B2 Scenario)
Depth of the Ocean (w_4)	Present (2009-17): http://www.buoyweather.com Future (2019 to 2070): http://worldclim.org/ (IPCC A2 and B2 Scenario)
Shipping Density (w_5)	Rank using the Density Map (http://www.marinetraffic.com/en/p/density-maps). A constant shipping density was assumed for the future scenarios
Percentage of Regular Waves (w_6)	The ratio of average of unidirectional wave and average of total number of wave in every 6 h was used for calculation of percentage regular waves. The data for baseline or 2009 to 2017 were retrieved from Buoyweather, and the future data (2019 to 2070) were estimated from World Clim data of Wind direction for both A2 and B2 scenarios
Direction of Wave (w_7)	The direction of wind speed as given in Buoyweather was assumed to be the direction of wave. A scoring system was used to quantify the indicator. The direction of wave perpendicular and toward the location was assumed to be the most sought-able direction for the production of wave energy and was assigned the maximum score of 10 and for each degree away from the perpendicular direction there will be a change of 1/9 points which will ultimately become zero when the direction of wave will be tangential to location of interest. The clockwise and anticlockwise change in direction was assumed to be assigned the same change in score as the impact of wave energy production does not change by the change in direction of waves from north to east or west. Wave direction for present or baseline scenario was collected from BuoyWeather and for the future scenario World Clim data were used
Average Wave Power Level of the Sea (w_8)	After collection of wave height (H_s) and period (T_e) data, Equation 4 was used for calculation of average wave power level (P_w), $P_w = \frac{\rho g^2}{64\pi} T_e H_s^2$ [4]
Corrosion (w_9)	Rating given by the group of experts out of a maximum score of ten where ten indicates maximum corrosive effect on the converter and zero indicates no corrosion. The experts analyzed the data of salinity of the location to decide about the score
Survivability (w_{10})	Rating given by the group of experts out of a maximum score of ten. The survivability is maximum when the score is ten and minimum when the score is zero. The experts analyzed the number of extreme events, heavy rainfall, storm surges, wind gusts, tsunami waves, etc., uncertainties to decide about the score. It can be assumed that more the frequency of these uncertainties, less will be the score for that location

(Continues)

TABLE 1 (Continued)

Name of parameter	Source/Method for data collection
Design aspects	
Size and Shape (Diameter, Draft, Displacement, Stroke Length, Height) (w_{11})	Specifications depicted in Brooke[5]
Mass of the Buoy (w_{12})	
Thickness of the Material Used(w_{13})	
Efficiency of Wave Rotor/Generator (w_{14})	
Efficiency of Turbine (w_{15})	
Efficiency of Energy Storage System (w_{16})	
Efficiency of Hydraulic System (w_{17})	
Power Conversion Efficiency at Constant or Nearly Constant RPM (w_{18})	
Cost aspect	
Installation Cost (INR) (w_{19})	Specifications depicted in Brooke[5]
Operation and Maintenance Costs (INR) (w_{20})	
External Costs (INR) (w_{21})	
Pre-Installation Cost (INR) (w_{22})	
Taxes (INR) (w_{23})	
Rate Per Unit of Electricity (INR) (w_{24})	

[a]Due to the impact of northerly or southerly wind, ocean waves of long length and steep height are found to be created in the ocean which are popularly known as a swell.[20,40,41] As both wave height and wave period are included as a parameter in the UEF, the swell created in the ocean can be represented by both of these two parameters.

Identification of the extreme events for the selected location was the third step of the present investigation. "In most cases, extreme events are defined as lying in the outermost ('most unusual') 10 percent of a place's history".[46] But the definition of "extreme event" varies with disciplines. In a study conducted on the definition of the extreme event, the authors[47] discussed in detail about this difference for disciplines such as "climatology, earth sciences, ecology, engineering, hydrology, and social sciences." As the present investigation is related to engineering discipline, identification of the extreme event was conducted as per the definition of the extreme events for engineering aspects and the procedure for the identification of extreme phenomena which can impact engineering designs followed by the methodology delineated by the authors for designing engineering infrastructures. Section 3.3 discusses about the identification of the extreme event with respect to the objective of the present investigation.

The results (estimated value of UEF) from the extreme event analysis were also validated with the help of an experimental setup (physical model) where a medium-scaled model[48] was developed having a Froude's scaling of 1/20 as the fourth step of the present study. All the relevant indicators were replicated into a laboratory flume following the same scaling to find the power output from the converter and the output was compared with the UEF to validate the interpretation from the value of the index. The experimental setup is shown in Figure 3A,B, and a brief description about the setup is included in Section 3.4. Figure 4 depicts the schematic of the methodology adopted in the present investigation for the analysis of extreme event impacts on utilization efficiency of selected WEC.

3.1 | Feature selection and data collection

In the present investigation, 24 indicators were used to estimate utilization efficiency function (UEF) for a wave energy converter (WEC). UEF is the index which represents the actual utilization of the wave energy potential of a location by a WEC.

The equation for the determination of UEF is depicted in Equation 1.

$$\text{UEF Index} = \frac{\sum W_n b_n}{\sum W_m \text{Nb}_m} \quad (1)$$

when $0 < W_n < 1, W_n \in \text{R}$ and $\text{m,n} \in \text{I}$

where W_n = priority value of tenth indicator representing the degree of positive influence by the indicator on the utilization efficiency of WEC.

W_m = priority value of the mth indicator depicting the degree of negative influence on the utilization efficiency of WEC.

b_n = magnitude of the nth indicator representing the degree of positive influence by the indicator on the utilization efficiency of WEC.

Nb_m = magnitude of the mth indicator depicting the degree of negative influence on the utilization efficiency of WEC.

m and *n* depict the maximum number of indicators considered in the study for the estimation of UEF, which have, respectively, positive and negative influences on the function, and R and I are the sets of real and integer numbers, respectively.

A PNN architecture with GMDH training algorithm was used to develop the predictive model for the estimation of UEF as a function of selected indicators. Equation 2 depicts the model equation. The detailed procedure of development of the model was described in the published work by Chakraborty and Majumder.[42,43]

$$\mathrm{UEF} = P(\mathrm{N_p}, b_n, \mathrm{Nb_m}) \tag{2}$$

$$b_n = F(w_1 \text{ to } w_{24} \text{ except } w_5, w_9, w_{19} \text{ to } w_{23}) \tag{2a}$$

$$\mathrm{Nb_m} = G(w_5, w_9, w_{19} \text{ to } w_{23}) \tag{2b}$$

The PNN model utilized for the estimation of UEF has 1 output, 83 numbers of hidden layers with 1011 nodes, and 24 numbers of inputs. N_p is the number of submodels of the polynomial neural network topology identified by the GMDH algorithm (Equation 2c).

$$\mathrm{N_2} = a_1 + \mathrm{N_{1009}^2} \times a_2 + \mathrm{N_3} \times a_3 \tag{2c}$$

where $a_1 = -2.76416$; $a_2 = 0.0887725$; $a_3 = 0.0999995$, and N_{1009} and N_3 can be found from Chakraborty and Majumder.[56,57]

Here, Equation 2a and 2b depict the beneficiary (b) and nonbeneficiary functions (Nb), which include the indicators which have, respectively, positive and negative influences on utilization efficiency of the converters. The P-function is the PNN function which was identified by the PNN architecture for the estimation of UEF by the input indicators. p indicates the maximum number of submodels of the PNN architecture identified by the GMDH algorithm for the estimation of the UEF with maximum reliability.

The input indicators of UEF comprise many factors which are sensitive to climatic parameters of a region. Like in the present study, all the location indicators (w_1 to w_{10}) except w_4, w_5, and w_9 are sensitive to the climatic parameters. Similarly, among all the cost indicator, w_{20} is sensitive to the climatic phenomena. The design indicator is not directly affected by the climatic parameters but is required to be adjusted as a response to the changes induced by a variation in the regular pattern of the climate or for the extreme events such that the utilization capability of the converters is not compromised. In case of the cost indicators, not only $w_{20,}$ remaining indicators were also affected indirectly by the "climate change."

The present study aims to analyze the impact of extreme events of the future on the actual utilization of wave energy potential by a WEC. But presently, there is no framework for the estimation of wave height in a location during the future time slabs. That is why in the present investigation, a simulation framework was developed to estimate wave height from wind speed as there are many models which is known as climate models which gives estimates of this climatic parameter for the future time slabs. Section 3.1.1 describes about one such climate model which is developed for the estimation of climatic parameters including wind speed in the location selected in the present study for impact analysis of extreme events on the utilization capacity of WEC.

3.1.1 | Climate prediction model: HadCM3

HadCM3 model was developed by Gordon et al[49] at the Hadley Centre in the United Kingdom which considered the influence of both atmospheric and oceanic parameters and includes the impact of aerosol on the climate. The model was widely used for different predictive studies such as estimation of climate change impact on groundwater recharge in arid regions of Iran,[50] water availability for different types of consumption in Tanzania,[51] water resources and soil erosion in Burkina Faso, West Africa,[52] paddy irrigation water requirements in Sri Lanka,[53] estimation of future distribution of plant species in the European continent,[54] and change in Arctic sea ice thickness and area for the future time slabs.[55] HadCM3 does not include flux adjustment due to its stable control climatology. The prediction of climate model is conducted for different climate change scenarios such as IPCC A1, A2, A1B, B1, and B2 as described in the third assessment report published by IPCC. As these scenarios were found to be more self-consistent compared to that of IS92 scenario, the prediction from HadCM3 was collected only for IPCC Special Report on Emission Scenario A2 and B2 scenario. The reason for exclusion of A1, A1B, and B1 and their subscenarios was due to the uncommonness of the scenarios with respect to the objective of the present study. Section 3.1.1.1 explains the scenarios A2 and B2 which were used in the present study for collection of predicted climatic data from the HadCM3 model.

IPCC A2 and B2 scenario

IPCC in its third assessment report has proposed four new scenarios which are more realistic and reliable compared to the earlier IS92 scenarios with respect to "socio-economic and emissions structure" which makes them more policy relevant compared to the previous scenarios.[56] In total, four main scenarios and two subscenarios were conceptualized

by the IPCC. In A2 scenario, heterogeneous world with increased industrialization was proposed and in case of B2 scenario increase in environmental stability was considered. The A1 and B1 scenarios predict an integrated and united world where industrialization and environmental stability are, respectively, encouraged. All these scenarios consider the continuous growth in population where rate of growth in A is higher compared to B-type scenarios.

In recent years, climatic data are generated based on the IPCC SRES scenario and used in various studies like for projecting future climate changes over upper Indus river basin,[57] to find the impact of future climate change on regional crop water requirement,[58] the analysis of impacts of climate change on various renewable energy resources,[59,60,61,62,63,64] and many other studies involving climate change impact analysis. In the present investigation, the impact of extreme events was analyzed for a location situated in Southern Indian peninsula. The geographical and climatic description of the selected location is described in Section 3.1.2.

3.1.2 | Study area

Kerala is located in the southern peninsula of Indian subcontinent. The state is surrounded by Karnataka in the north, Tamil Nadu in the east, and LakshaDweep Islands in the west. The state is located in the tropic region and has humid tropical wet climate. However, a dry climate is observed in the east and wettest region in Kerala including entire south India was observed in the southern part which is known as Malabar coastal region (MCR). The average annual rainfall of the state of Kerala was found to be 3107 mm. The coastal region of Kerala experiences a wind speed of 9.656 to 15.289 km/h, and maximum wind speed is generally observed within the month of May to October. The sampling region of the present study falls under Kochi (Figure 1) which is one of the windier places in India where the average wind speed varies between 7.564 and 12.392 km/h. The state has about 590 km long coastline in the country. The power potential per meter of wave crest was found to be equal to 20 KW in Kochi (100N, 760E) using the wave power equation proposed in Chakraborty and Majumder.[42,43] Figure 1 shows the location of the sampling points of the case study area.

The WEC selected for the analysis was Mighty Whale which is a type of oscillating water column (OWC) converter and utilized for electricity production in many places such as Japan, Norway, Scotland, Spain, Italy, India, and many other coastal region with a rigid shoreline structure. This type of converters is also most researched, and maximum number of modified prototypes is deployed in different oceans of the World.[65] Section 3.1.3 depicts a brief description about the Mighty Whale OWC WEC.

3.1.3 | Mighty whale wave energy converter

Mighty Whale [EMEC] is used as the prototype WEC for the present study.[44] This is a floating oscillating water column (OWC) type of wave energy converter device (Figure 2). It consists of an air turbine which is able to absorb the wave energy and convert to compressed air. The speed of this compressed air flow of air turbine drives the generator to convert the wave energy into electrical energy. Section 3.3 describes about the identification and selection of the extreme event impact of which will be analyzed with respect to the selected WEC, that is, Mighty Whale OWC WEC.

As depicted previously, a new simulation model was developed to estimate significant wave height as a function of wind speed. The procedure adopted to develop the model is explained in Section 3.3.

3.2 | Development of the simulation model used for the estimation of wave height

The significant wave height (SWH) was predicted with the help of a PNN model, trained with the GMDH algorithm, where input variable was selected as the function of wind speed. The function was derived from the inter-relationship of the parameter with the SWH. The data for training the model were collected from the wind speed and SWH data of the selected location for the last ten years. The mean monthly wind speed and SWH data were collected from the location. After normalization of the data set, the same is fed for training the model. 60% was used for training and 40% was utilized for testing or validating the model. After training, a 5-hidden layer with the same number of nodes was found to be the best topology for the estimation of the single input single output (SISO) model having an accuracy of 98% when compared with the projected data of SWH from the FORM technique.[45] Equation 3 depicts the governing equation of the model as estimated by the selected PNN architecture.

$$\mathrm{SWH} = [M + \{(A5 \times N) \times O + (-M + (N + A5 \times O) \times 1) \times Q\}] \quad (3)$$

where SWH is significant wave height (output variable) and $A5$ is the function (input variable).

$M = 0.00000000000226245; N = 0.00000000000427604$; $O = 0.2868$; $P = 0.491071$, $Q = 0.508929$.

The accuracy of the climate prediction varies with spatial resolution. That is why there are two types of climate prediction models, global and regional circulation models (GCM and RCM). The accuracy of the RCM is better compared to GCM due to the sharper spatial resolution of the former type of models. The applicability of RCM varies with locations or grids. In case of Asian grids, HadCM3 models are widely used and as the selected case study location is in the Asian continent, the future wind speed data were used in the present

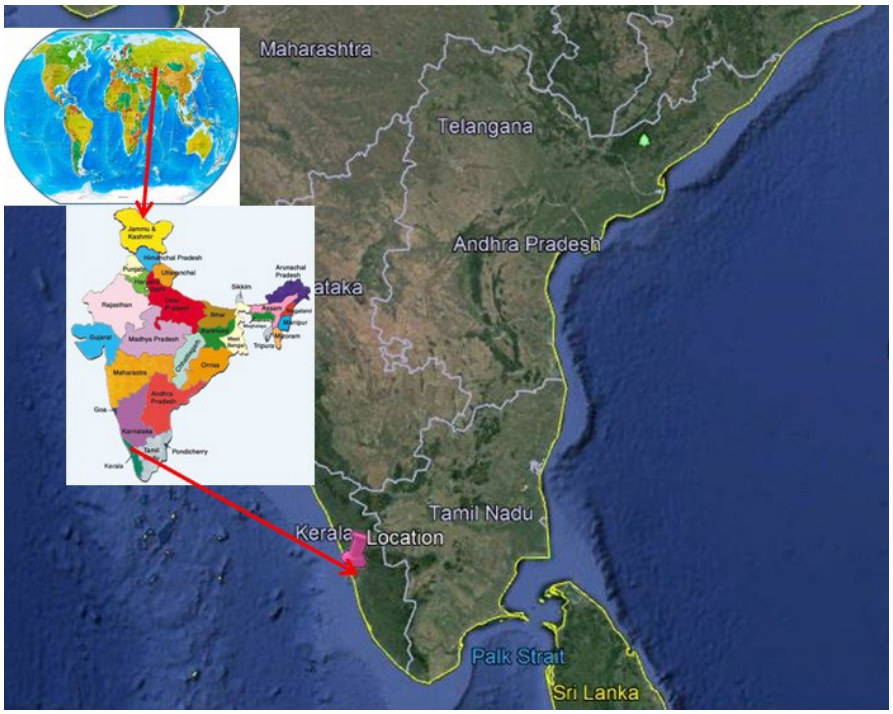

FIGURE 1 Figure showing the case study location

study to predict SWH by Equation 3. Section 3.3 describes about the climate model, and the climatic scenarios A2 and B2 are explained in Section 3.3.1.

3.3 | Identification of the extreme events

Among all types of WEC, it was found that a converter has a maximum lifetime of 25 to 30 years.[37] That is why in the present investigation the return periods were selected in such a way that two events each have a return period of more and less than 30 years, respectively, and one event was selected with 20 to 30 years of return period. Here, the events, which have more than 30 years of return period, fall below the 10% threshold for the identification of the extreme events, proposed in the definition by NOAA. The two events, which fall below the 30 years of return period, can be classified as common event and fall above the 10% threshold of all the events in the selected location. The event, which has 20 to 30 years of return period, falls within 10 to 30% of all the events. The reason for

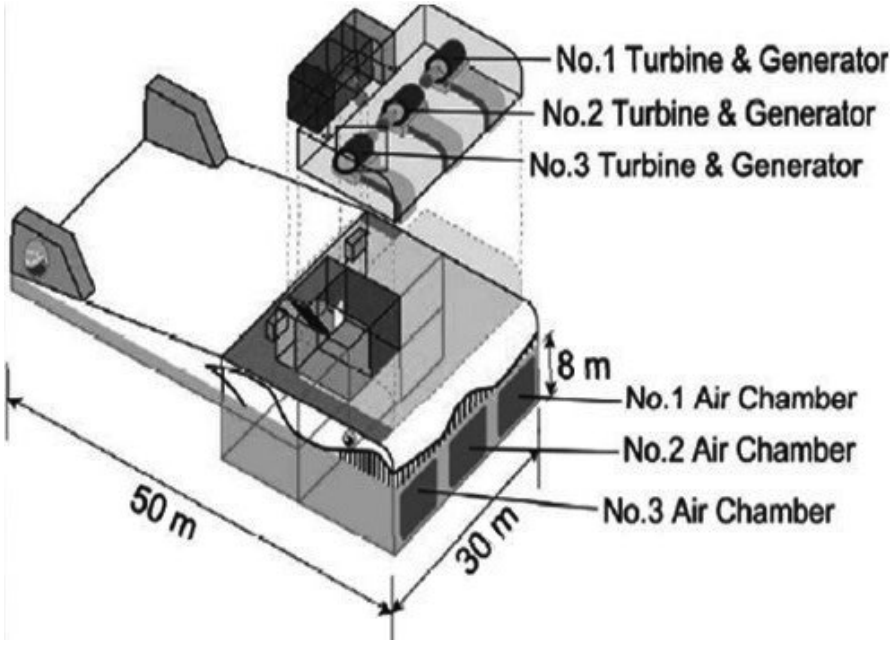

FIGURE 2 Schematic diagram of selected WEC (Source: International Energy Agency, 2018)

considering two common events along with two extreme events is to compare the impact of the extreme event with respect to the common events. The phenomena, which have 20 to 30 years of return period, were included in the study because any WEC has a lifetime of 30 years and a replacement is necessary when a converter is used for more than that period. That is why the impact for the events having 20 to 30 years of return period is important for practical conclusion of the impact analysis.

In the present investigation, the extreme event was calculated from the data of wind speed, retrieved from the selected climate model for both A2 and B2 scenarios. The event of wind speed was arranged in descending order of magnitude, and the return periods were calculated considering the variation to be normally distributed for each of the scenario. The events with 1 to 10 years, 10 to 20, 20 to 30, 30 to 50, and 50 to 60 years, were identified for each of the scenarios and fed to the simulation model (Equation 3) for the estimation of SWH. The wave period, direction of wave, and percentage of regular waves were estimated from the wind direction data retrieved from the World Clim climatic data center. Average wave power level for the future scenarios was estimated from the data of wave height and period of the future scenarios by Equation 4 (Table 1). Thus, five different UEF can be estimated for each of the A2 and B2 scenarios from the ten events collected from both A2 and B2 scenarios having a return period ranging from 1 to 60 years.

Once the extreme events were identified, the analysis was conducted by first predicting the UEF for the selected extreme events for both A2 and B2 scenarios. The UEF for the present condition was retrieved from the previous study of the authors of the present investigation. The predicted UEF was validated by a physical model where an experimental setup was developed to replicate the selected extreme events and monitoring the power output produced for such events. The entire procedure is depicted in Section 3.4.

3.4 | Experimental setup validation of the results from the impact analysis

The experimental setup was prepared to develop a physical model for validation of predicted UEF retrieved for different extreme events. Although the UEF index was compared with average wave power level of the selected locations for present climatic conditions,[42,43] the results were not validated for future climatic predictions, especially for the extreme events. In case of present scenario, available wave power data were used to validate the results from the UEF. But for the future time slabs, there are no primary or historical data for wave power and mostly estimation from simulations is used for decision-making considerations. That is why an experimental setup was established to validate the predicted UEF. In this aspect, a flume was designed as the base of the experiment. A piston was fixed at one end to act as the simulator of scenarios, and the dynamos were used to produce power and act as the output of the experiment. The detailed description of the experimental setup is depicted in 3.4.1.

3.4.1 | Description of the experimental setup

The entire experimental setup can be divided into flume, piston, and dynamos (Figure 3A). The dimension of the flume was 2 m × 2 m × 1 m. A piston was attached at the source end of the flume. Two concentrators were fixed in the left- and right-hand wall of the flume to channel the waves onto the dynamos. Three dynamos were arranged in series and placed at the focus of the concentrators. The waves, generated by the movement of the piston, flow into the concentrators and rotate the dynamos to produce power. After rotating the dynamos, water leaves the flume from the sink side and was recirculated by a motor to the source side. The same water is then used by the piston to generate waves. Three 100w dynamos were used in series to produce power due to the waves generated by the piston movement. The output of the dynamos was measured by a multimeter attached at the end connection of the last dynamo. The reason for using three dynamos was to multiply the power output from the dynamos. The loss due to resistance and reactance was included at the time of calculating efficiency which was assumed to represent the w_{14} to w_{18} indicators of the UEF. The wake effect due to the position of three dynamos in the flume was also included for the determination of efficiency.

Wave height and wave period that can be generated by the frequency of piston movement can be represented by Equations 5a and 5b in terms of the displacement in piston (x_p) and its capacity to generate waves of height H within a time t.

$$x_p(t) = \frac{H}{k}\left(\tanh x(t) + \tanh \frac{k}{d}\lambda\right) \tag{5a}$$

$$x(t) = \frac{k}{d}\left(ct - x_p(t) - \lambda\right) \tag{5b}$$

where H is the wave height, $k = \sqrt{\frac{3H}{4d}}$, and celerity, $c = \sqrt{g(d+H)}$, $x_p(t)$ is the displacement of the piston, d is the depth, $\lambda = \frac{d}{k}$

The percentage of regular wave, direction of wave, and average wave power level was also regulated by the piston. The percentage of regular waves can be estimated from the frequency of movements in the piston. The direction of the waves will be perpendicular to the direction of the piston movement. The average wave power level can be calculated by Equation 5 where the heights and period of the waves generated in the flume were used to determine the

average wave power level. The depth of the ocean waves was assumed to be equal to the depth of the flume which can be maximum of 1 m. The shipping density was kept at constant. Tax amount is also kept as constant. The dimension of the dynamos along with the concentrators was assumed to be representing the size and shape of the WEC. Here, dimension of the concentrator was equal to 0.5 m × 0.75 m × 0.05 m and made of steel in such a manner that minimum possible absorption of energy can be maintained.

The cost of the installation of flume, concentrators, dynamos, and the motor was considered as the installation cost. The cost incurred during the operation of the piston and dynamos including the expenditures due to maintenance was assumed to be equal to the operation and maintenance cost of the WEC. The cost of electricity charged by the local electricity regulator was assumed to be the rate of selling cost per unit electricity generated from the WEC (representing w_{24} indicator). The indicator tax was assumed to be constant. The indicators of UEF and its analogy in the experimental setup are depicted in Figure 3B.

The test was performed for five different frequencies of pistons replicating the wave height of five different extreme events. At first, the wind speed is converted to wave height by Equation 3. Then, the Equations 3a and 3b were used to find the frequency of piston movement required to generate the same wave height. Accordingly, this was operated, and the power generated due to the piston movement was noted from the multimeter for each of the scenarios. Corresponding UEF was also calculated and compared. The UEF was also compared with the power potential for these scenarios by the wave power equation proposed by Tucker and Pitt.[66] The three-phase validation of the UEF for the future time slabs

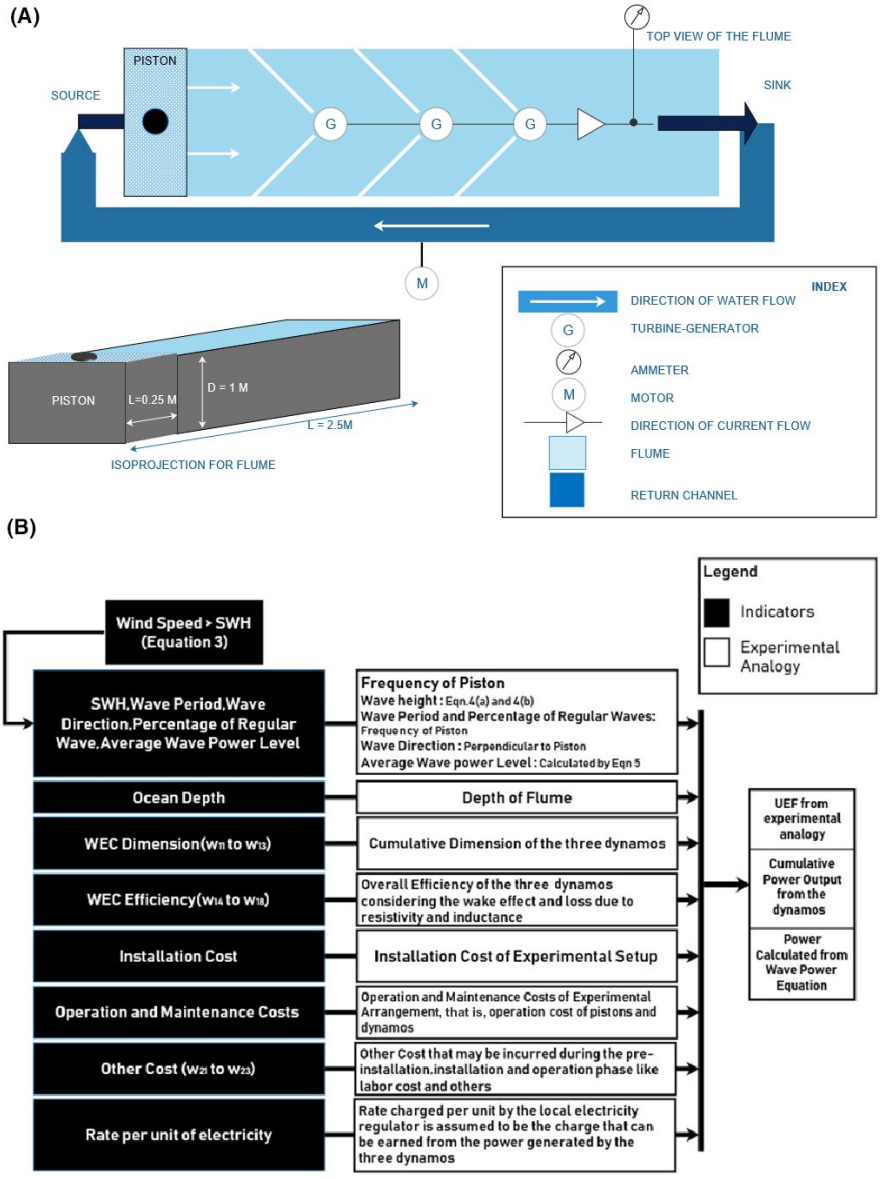

FIGURE 3 (A) Figure showing the experimental setup (B) Schematic diagram of experimental procedure

ensured reliability of the UEF estimations of the future time slabs.

The procedure adopted for replication of the events in the experimental setup is shown in Figure 3B. Section 4 describes the results retrieved following the methodology discussed in Section 3.

4 | RESULTS AND DISCUSSION

The objective of the present study was to estimate the impact of extreme events of the future on the utilization of wave energy potential by the selected WEC for a specific location. In this aspect, UEF was selected from the representation of the impact. The Kochi region of the Kerala coastal peninsula was identified as the location where Mighty Whale WEC was used as the WEC. Sections 4.1 to 4.4 give the results and discuss about the results retrieved from the steps: feature selection and data collection (Section 4.1), simulation model for SWH estimation from wind speed (Section 4.2), identification of the extreme events (Section 4.3), and lastly the prediction of UEF by Equation 2 followed by the validation of UEF by the physical model described in Section 4.4. A discussion on the impact of extreme event is included in Section 4.5.

4.1 | Results from the feature selection and data collection

The features or indicators selected for the present investigation are depicted in Table 1. All these indicators were selected for the estimation of UEF. The data for the indicators were collected for the selected case study area and WEC. The data were retrieved for the time slabs of 2009 to 2017 representing the current scenario and for the time slabs of 2019 to 2040 and 2040 to 2070 as the future scenario. Source and procedures of data collection are shown in Table 1.

The data for the future scenario were collected for both IPCC SRES A2 and B2 scenario and the same time slabs. As the climate models can estimate the climatic parameters only, the SWH was estimated from wind speed data collected from the HadCM3 model with the help of the simulation model. Results from the simulation model are described in Section 4.2.

4.2 | Results from the simulation model for the estimation of SWH from wind speed

Table 2 depicts the performance parameters of the polynomial neural network model developed with the help of GMDH training algorithm for the estimation of SWH from wind speed. The same estimation was conducted with the help of Quick Combinatorial training algorithm. Training data of the input and output were collected for the selected study area and from the Indian Meteorological Department (IMD) and Buoyweather, respectively, for the monthly average wind speed and wave data of 2009 to 2017. That is, 120 sets of data were used for the development of the SISO model. From the performance parameters, it can be clearly concluded that the GMDH-trained PNN model was better compared to QC-trained PNN model for the estimation of SWH. That is why the former model was used in the estimation of SWH from wind speed data.

The data for SWH were predicted for the future scenarios and compared with the data generated by the FORM

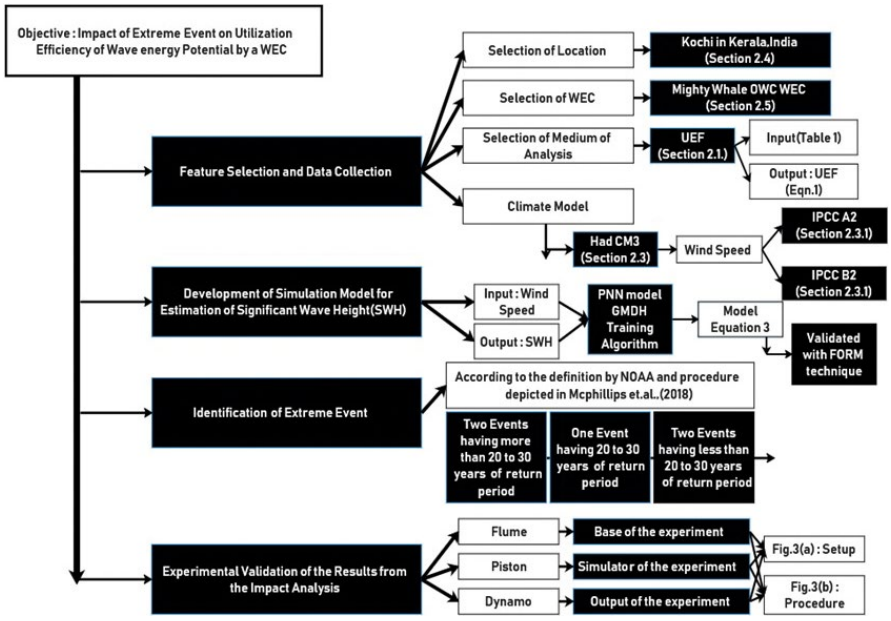

FIGURE 4 Schematics of the methodology adopted in the present study to analyze the impact of extreme events on utilization efficiency of WEC in a specific location

technique. The relative difference between the PNN-predicted SWH and FORM technique was found to be equal to 7.56%, and as this difference was below 20%, the model output was decided to be reliable.

4.3 | Identification of the extreme events

The extreme event for the present investigation was found by following the procedure recommended by McPhillips et al[47] The events were identified for both A2 and B2 scenarios. As discussed in Section 3.3, a total of five different extreme events were selected having a return period from 1 to 60 years. Table 3 depicts the percentage change in UEF and average wave power level (AWPL) from the UEF and AWPL of the current scenario with respect to the five extreme events identified for this study.

The most extreme events were found in 2060-2070 and 2050-2060, respectively, for the A2 and B2 scenarios. Table 3 displays that the AWPL decreases from the AWPL of the current scenario for both A2 and B2 scenarios with respect to all the five extreme events. The UEF value is also decreasing in both the scenarios. Maximum reduction of future UEF and AWPL in case of A2 scenario was identified in the year 2060-70 and was for the extreme event having a return period of 50 to 60 years. It was found that both UEF and AWPL will reduce by 15.10% and 61.39%, respectively, with respect to the current UEF and AWPL of Kochi region. The minimum decrease was found for the extreme event having a return period of 31 to 50 years where a reduction of 40.77% and 7.97% was found, respectively, for the AWPL and UEF compared to the current AWPL and UEF.

In case of B2 scenario, the maximum and minimum decrease of UEF and AWPL with respect to the current UEF and AWPL were found for the extreme event having a return period of 1 to 10 years. The amount of uppermost and lowermost reduction in UEF and AWPL was found to be equal to 10.38% and 50.71% and 6.67% and 40.45%, respectively.

The results clearly indicate that the increase in the return period of extreme events will decrease the UEF and corresponding AWPL for both A2 and B2 scenarios. However, magnitude of change will be more in A2 compared to B2 scenario. The reason can be attributed to the strict environmental policy considered in B2 scenario which will ensure a slow degradation in utilization by the WEC.

Once the extreme event was identified and the UEF was predicted by the UEF model (Equation 1), the predictions were validated by an experimental setup as described in Section 3.4. The results from the experimental analysis are depicted in Section 4.4.

4.4 | Results from the experimental validation of the UEF predicted for the future time slab

The power output from the medium-scaled physical model developed replicating the identified five extreme events along with the predicted UEF and AWPL for the scaled-down condition is shown in Tables 4 and 5, respectively, for the extreme events of A2 and B2 scenarios, which are identified in Section 3.3.

The change in UEF, wind speed, wave period, and SWH for the scaled-down physical model is shown in Figures 5 and

TABLE 2 Performance parameters of the polynomial neural network model developed with the help of GMDH training algorithm for the estimation of SWH from wind speed

Error measure (Absolute)	GMDH training algorithm		Quick combinatorial training algorithm	
	Model fit	Prediction	Model fit	Prediction
RMSE	1.43E-12	1.45 E-12	1.42 E-12	1.45 E-12
Correlation	1	1	1	1
Coefficient of determination	1	1	1	1

TABLE 3 Table showing the change in UEF and AWPL for the five extreme events identified for the present investigation from both A2 and B2 scenarios

Return period of the extreme events (year)	A2		B2	
	% change in AWPL	% change in UEF	% change in AWPL	% change in UEF
51-60	(−ve) 61.39	(−ve) 15.10	(−ve) 40.45	(−ve) 6.67
31-50	(−ve) 40.77	(−ve) 7.97	(−ve) 49.31	(−ve) 8.81
21-30	(−ve) 48.81	(−ve) 11.29	(−ve) 49.80	(−ve) 8.85
11-20	(−ve) 49.23	(−ve) 9.11	(−ve) 49.95	(−ve) 8.98
1-10	(−ve) 49.59	(−ve) 9.12	(−ve) 50.71	(−ve) 10.38

6, respectively, compared to the magnitude of the indicators with respect to the scaled-down model of the current scenario. Here, also maximum amount of change was observed in A2 scenario compared to B2 scenario which indicates that the predicted UEF for the future scenario is coherent with that of the scaled-down physical model. When the predicted UEF is scaled up, the average relative difference with the predicted UEF for all the five extreme events was found to be 3%, 42%, 43%, 41%, and 45%, respectively, for A2 and 19%, 0.5%, 41%, 42%, and 45%, respectively, for B2 scenarios.

The coherency and relative difference between the predicted UEF and scaled-down UEF indicate reliability of the prediction by the PEF model, and thus, impact analysis of the extreme event was conducted with the predicted UEF of the future and current scenario and is depicted in Section 4.5.

4.5 | Impact analysis of extreme event on the utilization of wave energy by the selected WEC

The magnitude of UEF was predicted with the help of the climatic data retrieved from the HadCM3 model collected for the IPCC SRES A2 and B2 scenario and is described in Section 3.1.1.

According to the results for the A2 scenario, there is a reduction of 15.1% in the UEF at A2 scenario. The highest percentage reduction in the UEF was found in the time slab of 2041 to 2070. The UEF was found to be degrading in B2 scenario also, and the maximum degradation of 10.38% was observed in the time slab of 2019 to 2040, although the intensity of the change is about 1.5 times less in B2 compared to A2 scenario. IPCC B2 scenario considers a divided world with strict environmental and ecological policy. The less decrease in UEF in B2 scenario compared to that in A2 scenario indicates the significance of the environmental restrictions which can result in greater utilization of the wave power potential by the WEC.

4.6 | Scientific benefits of the study

The UEF considers all the most significant indicators, which affect directly or indirectly the utilization efficiency of the converters, and as per their contribution, the evaluation of the magnitude of UEF helped to analyze the impact of extreme events on the "utilization efficiency" of the WEC by a single index only. The single-index evaluation reduces both time and cost of decision making. Another novel feature of the present study is the procedure of validation of the decision adopted based on the single-index method by a laboratory-based wave simulator specifically designed for the present investigation which can replicate the impact of extreme events on the WEC and compare with the modeled impact predicted by the UEF. This real-life validation of the model results increases the reliability of the present procedure proposed in the investigation. The novelty of the present study also includes the pioneering application of PNN model for the estimation of the impact of extreme events which was not adopted in any of the previous related studies.

TABLE 4 Table showing the experimental validation of UEF predicted for A2 scenario

Return period of the extreme events	Wind speed (m/s)	SWH (m)	UEF at the wind speed	Frequency of displacement (50 mg/s)	Power output from dynamo (mVA)	AWPL (kw/m)
51-60	4.31	2.77	1.21	7.75	0.015	5.80
31-50	4.01	2.57	1.12	7.23	0.013	3.45
21-30	3.99	2.56	0.86	7.20	0.013	3.35
11-20	3.99	2.56	0.95	7.19	0.013	3.48
1-10	3.96	2.54	1.15	7.15	0.012	3.28
Current scenario	4.85	2.89	1.05	8.09	0.025	5.98

TABLE 5 Table showing the experimental validation of UEF predicted for B2 scenario

Return period of the extreme events	Wind speed (m/s)	SWH (m)	UEF at the wind speed	Frequency of displacement (50 mg)/s	Power output from dynamo (mVA)	AWPL (kw/m)
51-60	4.04	2.17	1.12	6.12	0.010	4.80
31-50	3.94	2.76	1.01	7.75	0.015	5.95
21-30	3.93	2.57	1.11	7.23	0.013	3.49
11-20	3.93	2.56	1.05	7.20	0.013	3.46
1-10	3.91	2.56	1.148	7.19	0.013	3.26
Current scenario	4.85	2.89	1.05	8.09	0.025	5.98

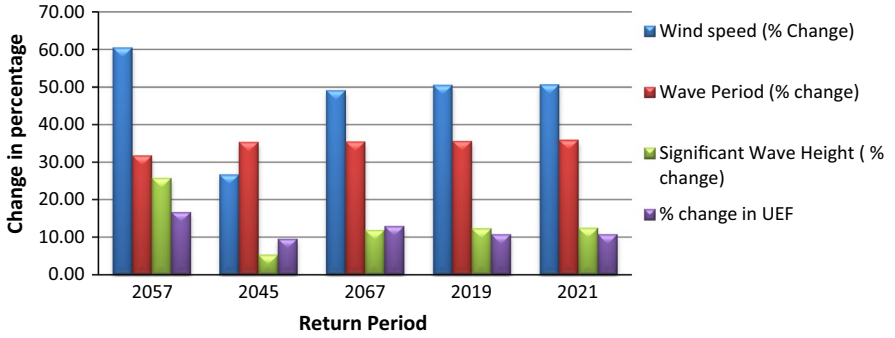

FIGURE 5 Figure showing the change in SWH, wave period, wind speed, and UEF with respect to the scaled-down model of A2 scenario compared to scaled-down model of current scenario

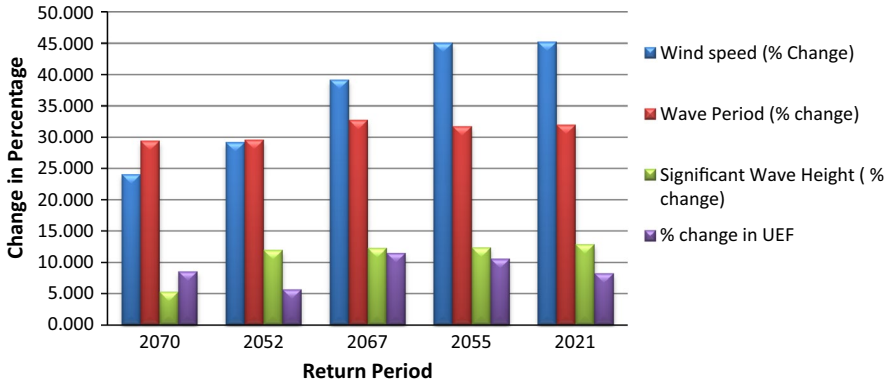

FIGURE 6 Figure showing the change in SWH, wave period, wind speed, and UEF with respect to the scaled-down model of B2 scenario compared to scaled-down model of current scenario

5 | CONCLUSION

The present investigation is a novel approach where the impact of extreme events on the utilization of wave power potential in a region by a WEC was analyzed. In this aspect, an index was selected which can represent the utilization of wave energy available in a location by a specific type of WEC. The index, UEF, is a function of 24 indicators most of which are affected by climatic parameters. As a result, if there is a change in the regular climatic pattern, the utilization of wave energy potential by the WEC will also be affected. That is why the study uses the UEF to depict the impact of extreme events on the utilization of wave power potential. The extreme events were identified for the A2 and B2 scenarios of future world as conceptualized by IPCC SRES. Before using UEF for the estimation extreme event impact, the future predictions were conducted by UEF model developed with the help of PNN architecture. The future prediction was validated with the help of a medium-scaled physical model where identified extreme events were replicated. Another model was developed to computationally simulate the SWH as a response to wind speed. As existing climate models predict future pattern of climatic variables only, the requirement of a new model for the estimation of SWH from the climatic parameters becomes essential for impact analysis of climate change. PNN architecture was again used to develop the model. After all the data for current and present scenarios of the 24 indicators were collected, UEF was estimated for the five different extreme events for both A2 and B2 scenarios. According to the results of the prediction, utilization by WEC will be reduced in the future time slabs; however, the degradation will be much higher in A2 compared to B2 scenario, which shows the importance of environmental restriction on industrial activity that ensures milder degrading impact on the utilization of wave energy potential by the WEC. The maximum degradation was found in the time slab of 2041 to 2070 in A2 scenario, but for B2 scenario, the highest decrease in UEF was observed in the initial years of strict environmental restrictions, that is, in the 2019 to 2040 time slabs. As later on, the situation improves and so is the decrease in utilization. Although a physical model is used to validate the model predictions, due to the large number of inputs, collection of pertinent data and impact of all the inputs may reduce the usability of the model. However, a sensitivity analysis or activating self-selection capability of GMDH algorithms can separate essentially from optional inputs and thereby decreasing the time required in preprocessing of the predictive procedure and can increase the accuracy of the model.

ORCID

Mrinmoy Majumder https://orcid.org/0000-0001-6231-5989

REFERENCES

1. ATMOCEAN. The Potential of Wave Energy; 2018. Retrieved from https://atmocean.com/the-potential-of-wave-energy/

2. A comprehensive annual overview of the state of renewable energy (2019). REN 21 "Renewables 2018-Global status report."
3. Owusu PA, Asumadu-Sarkodie S. A review of renewable energy sources, sustainability issues and climate change mitigation. *Cogent Eng*. 2016;3(1):1167990.
4. Ransley EJ, Greaves D, Raby A, Simmonds D, Hann M. Survivability of wave energy converters using CFD. *Renew Energy*. 2017;109:235-247.
5. Brooke J. *Wave Energy Conversion*, Vol. 6. Amsterdam, Netherlands: Elsevier; 2003.
6. Wang W, Wu M, Palm J, Eskilsson C. Estimation of numerical uncertainty in computational fluid dynamics simulations of a passively controlled wave energy converter. *Proc IME M J Eng Marit Environ*. 2018;232(1):71-84.
7. Hughes MG, Heap AD. National-scale wave energy resource assessment for Australia. *Renew Energy*. 2010;35(8):1783-1791.
8. Aboobacker VM, Shanas PR, Alsaafani MA, Albarakati AMA. Wave energy resource assessment for Red Sea. *Renew Energy*. 2017;114:46-58.
9. Re CL, Manno G, Ciraolo G, Besio G. Wave energy assessment around the Aegadian Islands (Sicily). *Energies*. 2019;12(3):333.
10. Sasmal K, Webb A, Waseda T, Miyajima S. Wave energy resource assessment: A comparative study for two coastal areas in Japan. In *Advances in Renewable Energies Offshore: Proceedings of the 3rd International Conference on Renewable Energies Offshore (RENEW 2018), October 8-10, 2018, Lisbon, Portugal*, p. 67. CRC Press; 2018.
11. Lin Y, Dong S, Wang Z, Guedes Soares C. Wave energy assessment in the China adjacent seas on the basis of a 20-year SWAN simulation with unstructured grids. *Renew Energy*. 2019;136:275-295.
12. Chakraborty T, Majumder M, Khare A. Application of AHP-VIKOR and GMDH framework to develop an indicator to identify utilisation potential of wave energy converter with respect to location. *Int J Spatio-Temporal Data Sci*. 2019;1(1):98-113.
13. Zanous SP, Shafaghat R, Alamian R, Shadloo MS, Khosravi M. Feasibility study of wave energy harvesting along the southern coast and islands of Iran. *Renew Energy*. 2019;135:502-514.
14. Castelle B, Dodet G, Masselink G, Scott T. Increased winter-mean wave height, variability, and periodicity in the Northeast Atlantic over 1949-2017. *Geophys Res Lett*. 2018;45:3586-3596.
15. Zheng CW, Gao ZS, Liao QF, Pan J. Status and prospect of the evaluation of the global wave energy resource. *Recent Patents Eng*. 2016;10(2):98-110.
16. Danovaro R. Climate change impacts on the biota and on vulnerable habitats of the deep Mediterranean Sea. *Rendiconti Lincei. Scienze Fisiche e Naturali*. 2018;29(3):525-541.
17. Sisco MR, Bosetti V, Weber EU. When do extreme weather events generate attention to climate change? *Clim Change*. 2017;143(1–2):227-241.
18. Acuna LG, Vasquez Padilla R, Mercado AS. Measuring reliability of hybrid photovoltaic-wind energy systems: a new indicator. *Renew Energy*. 2017;106:68-77.
19. Liu G, Li M, Zhou B, Chen Y, Liao S. General indicator for techno-economic assessment of renewable energy resources. *Energy Convers Manage*. 2018;156:416-426.
20. Zheng CW, Wang Q, Li CY. An overview of medium-to long-term predictions of global wave energy resources. *Renew Sustain Energy Rev*. 2017;79:1492-1502.
21. Reguero BG, Losada IJ, Méndez FJ. A global wave power resource and its seasonal, interannual and long-term variability. *Appl Energy*. 2015;148:366-380.
22. Seneviratne SI, Nicholls N, Easterling D, et al. *Changes in Climate Extremes and Their Impacts on the Natural Physical Environment*. Cambridge: Cambridge University Press; 2012.
23. Ulazia A, Penalba M, Ibarra-Berastegui G, Ringwood J, Saénz J. Wave energy trends over the Bay of Biscay and the consequences for wave energy converters. *Energy*. 2018;141:624-634.
24. Wabnitz CC, Lam VW, Reygondeau G, et al. Climate change impacts on marine biodiversity, fisheries and society in the Arabian Gulf. *PLoS ONE*. 2018;13(5):e0194537.
25. Zheng CW, Li C, Wu H, Wang M. Climatic trend and prediction of the wind energy in the Gwadar Port. In: *21st Century Maritime Silk Road: Construction of Remote Islands and Reefs*. Singapore City: Springer; 2018:35-57.
26. Jiang L, Yin Y, Cheng X, Zhang Z. Interannual variability of significant wave height in the northern South China Sea. *Aquat Ecosyst Health Manage*. 2018;21(1):82-92.
27. Mori N, Shimura T, Yasuda T, Mase H. Multi-model climate projections of ocean surface variables under different climate scenarios—future change of waves, sea level and wind. *Ocean Eng*. 2013;71:122-129.
28. Nguyen XH, Dinh VU, Tran VT. Impacts of climate change on wave regimes in the east sea. *Vietnam J Sci Technol Eng*. 2017;59(1):88-92.
29. Regos A, Clavero M, D'amen M, Guisan A, Brotons L. Wildfire–vegetation dynamics affect predictions of climate change impact on bird communities. *Ecography*. 2018;41(6):982-995.
30. Ruffato-Ferreira V, da Costa Barreto R, Oscar Júnior A, et al. A foundation for the strategic long-term planning of the renewable energy sector in Brazil: hydroelectricity and wind energy in the face of climate change scenarios. *Renew Sustain Energy Rev*. 2017;72:1124-1137.
31. Hillebrand H, Brey T, Gutt J, et al. Climate change: warming impacts on marine biodiversity. In: Salomon M, Markus T, eds. *Handbook on Marine Environment Protection*. Cham: Springer; 2018:353-373.
32. Hoegh-Guldberg O, Bruno JF. The impact of climate change on the world's marine ecosystems. *Science*. 2010;328(5985):1523-1528.
33. IEA. World Energy Outlook; 2017. Retrieved from https://www.iea.org/weo2017/ on 13 October 2018.
34. IMHEN. Applying Norwegian earth system model for Climate Change scenario development for Vietnam, monsoon and climate extreme studies, Final report, Hanoi; 2014.
35. Kamranzad B, Etemad-Shahidi A, Chegini V, Yeganeh-Bakhtiary A. Climate change impact on wave energy in the Persian Gulf. *Ocean Dyn*. 2015;65(6):777-794.
36. Keigwin LD, Change AC, Climates P. Sedimentary record yields several centuries of data. *Life*. 2018;2:16-19.
37. Coe RG, Neary VS. *Review of Methods for Modeling Wave Energy Converter Survival in Extreme Sea States*. New Mexico, USA: U.S. Department of Energy; 2014.
38. Tu F, Ge SS, Choo YS, Hang CC. Sea state identification based on vessel motion response learning via multi-layer classifiers. *Ocean Eng*. 2018;147:318-332.
39. Ghosh S, Chakraborty T, Saha S, Majumder M, Pal M. Development of the location suitability index for wave energy production

by ANN and MCDM techniques. *Renew Sustain Energy Rev*. 2016;59:1017-1028.
40. Ardhuin F, Marie L, Rascle N, Forget P, Roland A. Observation and estimation of Lagrangian, Stokes, and Eulerian currents induced by wind and waves at the sea surface. *J Phys Oceanogr*. 2009;39(11):2820-2838.
41. Remya PG, Vishnu S, Praveen Kumar B, Balakrishnan Nair TM, Rohith B. Teleconnection between the North Indian Ocean high swell events and meteorological conditions over the Southern Indian Ocean. *J Geophys Res Oceans*. 2016;121(10):7476-7494.
42. Chakraborty T, Majumder M. Application of non-parametric and cognitive modelling for development of location selection indicator for wave energy converters. *Int J Control Theory Appl*. 2017a;10:1-21.
43. Chakraborty T, Majumder M. Application of statistical charts, multi-criteria decision making and polynomial neural networks in monitoring energy utilization of wave energy converters. *Environ Dev Sustain*. 2017b;21(1):1-21.
44. Wu B, Chen T, Jiang J, Li G, Zhang Y, Ye Y. Economic assessment of wave power boat based on the performance of "Mighty Whale" and BBDB. *Renew Sustain Energy Rev*. 2018;81:946-953.
45. Winterstein SR, Ude TC, Cornell CA, Bjerager P, Haver S. Environmental parameters for extreme response: Inverse FORM with omission factors. Proceedings of the ICOSSAR-93, Innsbruck, Austria, 551-557; 1993.
46. NOAA. Extreme Event, National Center for Environment Information; 2018. Retrieved from https://www.ncdc.noaa.gov/climate-information/extreme-events on 19 December 2018.
47. McPhillips LE, Chang H, Chester MV, et al. Defining extreme events: a cross-disciplinary review. *Earth's Future*. 2018;6(3):441-455.
48. Holmes B, Nielsen K. *Guidelines for the Development & Testing of Wave Energy Systems*. Lisbon, Portugal: International Energy Agency Ocean Energy Systems; 2010.
49. Gordon C, Cooper C, Senior CA, et al. The simulation of SST, sea ice extents and ocean heat transports in a version of the Hadley Centre coupled model without flux adjustments. *Clim Dyn*. 2000;16(2–3):147-168.
50. Ghazavi R, Ebrahimi H. Predicting the impacts of climate change on groundwater recharge in an arid environment using modeling approach. *Int J Clim Chang Strat Manage*. 2019;11(1):88-99.
51. Kishiwa P, Nobert J, Kongo V, Ndomba P. Assessment of impacts of climate change on surface water availability using coupled SWAT and WEAP models: case of upper Pangani River Basin, Tanzania. *Proc Int Assoc Hydrol Sci*. 2018;378:23-27.
52. de Hipt FO, Diekkrüger B, Steup G, Yira Y, Hoffmann T, Rode M. Modeling the impact of climate change on water resources and soil erosion in a tropical catchment in Burkina Faso, West Africa. *Catena*. 2018;163:63-77.
53. De Silva CS, Weatherhead EK, Wo Knox J, Rodriguez-Diaz JA. Predicting the impacts of climate change—a case study of paddy irrigation water requirements in Sri Lanka. *Agric Water Manag*. 2007;93(1–2):19-29.
54. Thuiller W. Patterns and uncertainties of species' range shifts under climate change. *Glob Change Biol*. 2004;10(12):2020-2027.
55. Gregory JM, Stott PA, Cresswell DJ, Rayner NA, Gordon C, Sexton DMH. Recent and future changes in Arctic sea ice simulated by the HadCM3 AOGCM. *Geophys Res Lett*. 2002;29(24):28-1 to 28-4.
56. Johns TC, Gregory JM, Ingram WJ, et al. Anthropogenic climate change for 1860 to 2100 simulated with the HadCM3 model under updated emissions scenarios. *Clim Dyn*. 2003;20(6):583-612.
57. Khattak MS, Babel MS, Khan TA, Sharif M, Khalil SA. Global climate model for projecting future climate changes over upper Indus River Basin. *Pak J Agri Agri Eng Vet Sci*. 2017;33(2):227-242.
58. Zhou T, Wu P, Sun S, Li X, Wang Y, Luan X. Impact of future climate change on regional crop water requirement—a case study of Hetao Irrigation District, China. *Water*. 2017;9(6):429.
59. Carvalho D, Rocha A, Gómez-Gesteira M, Silva Santos C. Potential impacts of climate change on European wind energy resource under the CMIP5 future climate projections. *Renew Energy*. 2017;101:29-40.
60. Davy R, Gnatiuk N, Pettersson L, Bobylev L. Climate change impacts on wind energy potential in the European domain with a focus on the Black Sea. *Renew Sustain Energy Rev*. 2018;81(P2):1652-1659.
61. de Oliveira Tiezzi R, Vieira NDB, Simoes AF, et al. Impacts of climate change on hydroelectric power generation–a case study focused in the Paranapanema Basin, Brazil. *J Sustain Dev*. 2018;11(1):140.
62. Hdidouan D, Staffell I. The impact of climate change on the levelised cost of wind energy. *Renew Energy*. 2017;101:575-592.
63. Mann ME, Rahmstorf S, Kornhuber K, Steinman BA, Miller SK, Coumou D. Influence of anthropogenic climate change on planetary wave resonance and extreme weather events. *Sci Rep*. 2017;7:45242.
64. Sierra JP, Casas-Prat M, Campins E. Impact of climate change on wave energy resource: the case of Menorca (Spain). *Renew Energy*. 2017;101:275-285.
65. Falcao AFO, Henriques JCC. Oscillating-water-column wave energy converters and air turbines: a review. *Renew Energy*. 2016;85:1391-1424.
66. Brooke J. Wave Energy Conversion System *Wave Energy Conversion System, Volume 6*, Oxford, UK: Elsevier; 2003:27-32.

How to cite this article: Chakraborty T, Majumder M. Impact of extreme events on conversion efficiency of wave energy converter. *Energy Sci Eng*. 2020;8:3441-3456. https://doi.org/10.1002/ese3.336